photonics

MDPI

Article

Numerical Analysis and Verification of Off-Axis Double Vortex Beams

Jianqiang Ye [1], Yuxia Zhou [1,2], Palidan Aierken [1], Xining Yang [1], Zhaoxue Li [1,*] and Taximaiti Yusufu [1,*]

[1] Xinjiang Key Laboratory for Luminescence Minerals and Optical Functional Materials, School of Physics and Electronic Engineering, Xinjiang Normal University, Urumqi 830054, China; a642226834@gmail.com (J.Y.); zhou_yx0801@sina.com (Y.Z.); palidan2019@163.com (P.A.); yangxn1984@126.com (X.Y.)
[2] School of Chemistry and Chemical Engineering, Xinjiang Normal University, Urumqi 830054, China
* Correspondence: zhaoxue_l@163.com (Z.L.); taxmamat_84@sina.com (T.Y.)

Abstract: Vortex beams are unique in that they have annular spatial profiles and carry orbital angular momentum. This has led to their use in applications including laser processing, microparticle manipulation and signal transmission. Off-axis vortex beams, which may be considered a subset of vortex beams, display a broader spectrum of physical characteristics in comparison with their conventional (integer-order) counterparts. In this work, we derive the equations which describe the intensity distribution of off-axis vortex beams and use these to theoretically model their spatial profile. These models are supported by experimental generation of both integer and off-axis vortex beams, and the presence of orbital angular momentum is investigated through the use of the cylindrical lens transformation method.

Keywords: laser technology; optical vortex; off-axis double vortex beam; spiral phase plate

1. Introduction

As established by Allen et al. [1], one of the defining characteristics of vortex beams is that they have a phase singularity and carry orbital angular momentum (OAM). Here, vortex beams have a characteristic phase term, $\exp(il\theta)$, wherein l represents the order of orbital angular momentum, or equivalently the topological charge, and θ represents the azimuthal angle in cylindrical coordinates. The unique characteristics of OAM and how it can be imparted to physical media have led to significant interest in vortex beams and, more generally, their methods of generation and application. In recent years, numerous methods have been used for the generation of vortex beams using devices, such as spiral phase plates (SPP) [2], Q-plates [3], fiber lasers [4–6], spatial light modulators (SLM) [7], and digital micromirror devices (DMD) [8]. These have been used to generate vortex beams, including integer-order vortex beams [9,10], fractional-order vortex beams [11,12], elliptical vortex beams [13,14], and so-called "perfect vortex beams" [15,16]. Concurrently, a considerable body of research has focused on the extension of the spectral range covered by vortex beams [17–24]. Researchers have also extensively studied the physical properties of vortex beams and applied them in fields including particle manipulation [25], optical communication [26,27], quantum communication [28,29], high-resolution microscopy [30,31], terahertz polarization detection [32,33], material processing [34,35], and optical measurements [36].

There exist sub-sets of vortex beams, such as fractional vortex beams; these are vortex beams which have non-integer OAM and can be generated through the use of a non-integer spiral phase step [37,38]. Off-axis vortex beams are another sub-set of vortex beams which have spatial forms which have a radial opening and can be described as a coherent superposition of Laguerre–Gaussian (LG) laser modes [39]. In comparison to traditional optical vortex beams, non-integer and off-axis vortex beams with states of non-integer OAM can be applied to unique and exotic light–matter interactions, such as sorting and directional control of living cells [40], due to the property of the annular structure of the

check for updates

Citation: Ye, J.; Zhou, Y.; Aierken, P.; Yang, X.; Li, Z.; Yusufu, T. Numerical Analysis and Verification of Off-Axis Double Vortex Beams. *Photonics* **2024**, *11*, 123. https://doi.org/10.3390/photonics11020123

Received: 7 December 2023
Revised: 22 January 2024
Accepted: 26 January 2024
Published: 29 January 2024

off-axis double vortex beam being broken. It is therefore possible to make more delicate manipulations on these particles. Also, these beams can be used to significantly increase the data capacity of optical communication systems and enable spatial entanglement with infinite-dimensional subspaces in quantum optics [41]. Techniques used for the generation of such vortex beams include using external phase control components, such as SLMs [42].

When generating vortex beams, it is generally desirable to produce beams wherein the phase singularity is positioned perfectly within the center of the beam. However, it is often observed that vortex beams which are experimentally generated using SPPs, fork gratings and SLMs have alignment errors (which manifest due to positioning and fabrication errors), causing the phase singularity to deviate from the axis of the beam, yielding off-axis vortex beams. Compared with traditional, symmetric vortex beams, off-axis/asymmetric vortex beams contain a higher level of complexity. This characteristic means these beams can be exploited for applications, such as communications wherein the beams can carry greater information density and applications in manipulation where higher degrees of freedom can be achieved [43–45]. In comparison to off-axis, single vortex beams (which have one phase singularity), off-axis double vortex beams (which have two phase singularities) have even greater complexity. There has been relatively little research on off-axis double vortex beams, and a complete description of their optical fields is still lacking.

Typically, the generation of exotic or complex beam shapes proceeds from the derivation of equations, the determination of appropriate holographic grating profiles and then the loading of these profiles onto an SLM for the generation of the desired beam shape [45]. The accuracy and characteristics of the generated beam shape hence depend critically on the correctness of the applied equations and the quality and accuracy of the SLM. In contrast to this approach, in this work, we utilize the superposition of two SPPs (optical elements which can be fabricated with a high degree of accuracy) to generate off-axis vortex beams. Using this approach, we can better ensure the accuracy and correctness of both the generated beam and the equations describing these beams. We are able to observe the whole change process of the beam by changing the off-axis displacement between two SPPs and verifying the beam morphology and orbital angular momentum well by intensity distribution and the cylindrical lens convergence method. Then, we compare it with the simulation diagram made by equations to examine the correctness of the equations.

This paper commences with the equation describing integer-order vortex beams and this is used to derive the amplitude distribution equation for off-axis double vortex beams. The correctness of these derivations is then verified experimentally where we generate a range of integer-order and off-axis vortex beams. When the off-axis position of the optical singularity is 0, the equation degenerates into an equation describing integer-order vortex beams, and when the sum of l_1 and l_2 equals 0, it degenerates into the equation describing a Gaussian beam. We also investigate the presence of OAM through the use of the cylindrical lens transformation method; it is verified that when off-axis displacements destroy the toroidal structure of vortex beams, which can also carry partial orbital angular momentum (non-integer) and be stably transmitted, these beams may be of great use in high-density communication and higher-order microoperation applications.

2. Theoretical Derivation of Off-Axis Double Vortex Beams

We derive the equation describing the amplitude of an off-axis double vortex beam from the equation describing an integer-order vortex beam. From this, we theoretically model the spatial intensity distribution of the beams and the transformed beam patterns (on propagation through a cylindrical lens). These intensity distributions are then compared with experimentally obtained results.

The equation describing the amplitude of an integer-order vortex beam can be derived from Helmholtz simulations [46,47]. A unique property of integer-order vortex beams is that they have a symmetric spatial intensity profile and they stably propagate in free space [48]. The angular momentum of these beams is dictated by $\exp(il\theta)$, with l signifying the order of OAM, which must be an integer [49]. Off-axis beams, in contrast, have

an asymmetric distribution, can have non-zero angular momentum and exhibit stable propagation in free space.

The electric field amplitude of integer-order vortex beams can be described as follows [50]:

$$E_{VB} = \left(\frac{\sqrt{2}r}{\omega_z}\right)^{|l|} \cdot \exp\left(-\frac{r^2}{\sqrt{2}\omega_z}\right) \times \exp(i \cdot l \cdot \theta) \tag{1}$$

where the amplitude of $(\sqrt{2}r/\omega_z)^{|l|}$ is responsible for the beam intensity and phase $\exp(il\theta)$ accounts for the OAM. Through the aforementioned two light field influencing factors, further modifications are made to the formula (by embedding another factor, corresponding to the role of SPP2 in the experiment). We produce an off-axis double vortex beam by introducing the "reference factor" and the "embedded factor", corresponding to SPP1 and SPP2, respectively. The reference factor (SPP1) was fixed and the embedded factor was adjusted by moving the SPP2, where l_1 and l_2, respectively, correspond to the OAM orders of the " embedded factor " and the " reference factor ". After these treatments, the description equation for off-axis double vortex beams can be obtained. A slight off-axis displacement of the beam can be accommodated with the following modification to the equation:

$$\begin{aligned} E_{OAVB} = &\left(\frac{\sqrt{2}\cdot\sqrt{(x-\Delta x)^2+(y-\Delta y)^2}}{\omega_z}\right)^{|l_1|} \cdot \left(\frac{\sqrt{2}r}{\omega_z}\right)^{|l_2|} \cdot \exp\left(-\frac{r^2}{\sqrt{2}\omega_z}\right) \\ &\times \exp\left(i \cdot l_1 \cdot \operatorname{atan}\left(\frac{y-\Delta y}{x-\Delta x}\right)\right) \times \exp\left(i \cdot l_2 \cdot \operatorname{atan}\left(\frac{y}{x}\right)\right) \end{aligned} \tag{2}$$

where Δx and Δy represent the displacements of the embedded factor in the X and Y directions, respectively, relative to the reference factor. It should be noted that when $l_1 \times l_2 < 0$, the intensity distribution is no longer accurate. For example, when $l_1 = 1$, $l_2 = -1$ and the off-axis displacement is 0, the intensity distribution will be a ring distribution, which is the same as the 2nd-order optical vortex ground intensity distribution but does not carry orbital angular momentum. (This is obviously incorrect.) Therefore, we introduce the following supplementary equation:

$$\begin{aligned} E_{OAVB} = &\left(\frac{\sqrt{2}\cdot\sqrt{(x-\Delta x)^2+(y-\Delta y)^2}}{\omega_z}\right)^{l_1} \cdot \left(\frac{\sqrt{2}r}{\omega_z}\right)^{l_2} \cdot \exp\left(-\frac{r^2}{\sqrt{2}\omega_z}\right) \\ &\times \exp\left(i \cdot l_1 \cdot \operatorname{atan}\left(\frac{y-\Delta y}{x-\Delta x}\right)\right) \times \exp\left(i \cdot l_2 \cdot \operatorname{atan}\left(\frac{y}{x}\right)\right) \times \exp(i \cdot k \cdot z) \end{aligned} \tag{3}$$

When both Δx and Δy are equal to 0, the equation degenerates to the following:

$$E_{OAVB} = \left(\frac{\sqrt{2}r}{\omega_z}\right)^{l_1+l_2} \cdot \exp\left(-\frac{r^2}{\sqrt{2}\omega_z}\right) \times \exp[i \cdot (l_1 + l_2) \cdot \theta] \tag{4}$$

This equation is almost identical to the equation describing integer-order vortex beams. The intensity distribution of the beam can be obtained from

$$I_{OAVB} = E_{OAVB} \cdot E^*_{OAVB} \tag{5}$$

Equations (2), (3) and (5) were used in our theoretical calculations/models.

3. Experimental Results

In this work, we used the superposition of two SPPs to experimentally generate off-axis vortex beams. Such an approach is valid as the first SPP, SPP2, imparts an orbital angular momentum, l_1, to the laser field, and SPP1 imparts an orbital angular momentum l_2. As such, we utilize a number of SPPs, each fabricated to provide values $l_1 = -1$ and $l_1 = 1$ and $l_2 = 0, 1, 2, 3, 4$. By adjusting the position of SPP2 (both in X and Y directions), the position of the embedding factor can be adjusted to produce off-axis displacements (corresponding to Δx and Δy in the equation). These SPPs azimuthally divided into 16 segments. The

experimental setup is shown in Figure 1. The laser source was a conventional Q-switched Nd:YAG laser (LS-2036, pulse duration of 25 ns, PRF of 50 Hz) producing an output with a Gaussian spatial profile at a wavelength of 1064 nm. The spatial form of the vortex beams was characterized using a conventional CCD camera. SPP1 was used to first generate a conventional vortex beam. By adjusting the off-axis (in X and Y directions) position of SPP2 relative to SPP1, we were able to generate off-axis double vortex beams. The intensity distribution of the beams depended on the relative off-axis displacement between the two SPPs. When the off-axis displacement was small but finite, the spatial distribution of the vortex beam became asymmetric (and characteristic of an off-axis vortex beam). As this off-axis displacement became greater (exceeding that of the radius of the beam), the effect of SPP2 diminished. For each generated beam, its OAM content was determined using the cylindrical lens transformation method. Also, each beam shape was modelled using the equations derived in the previous section, and the simulations were compared with the experimental results.

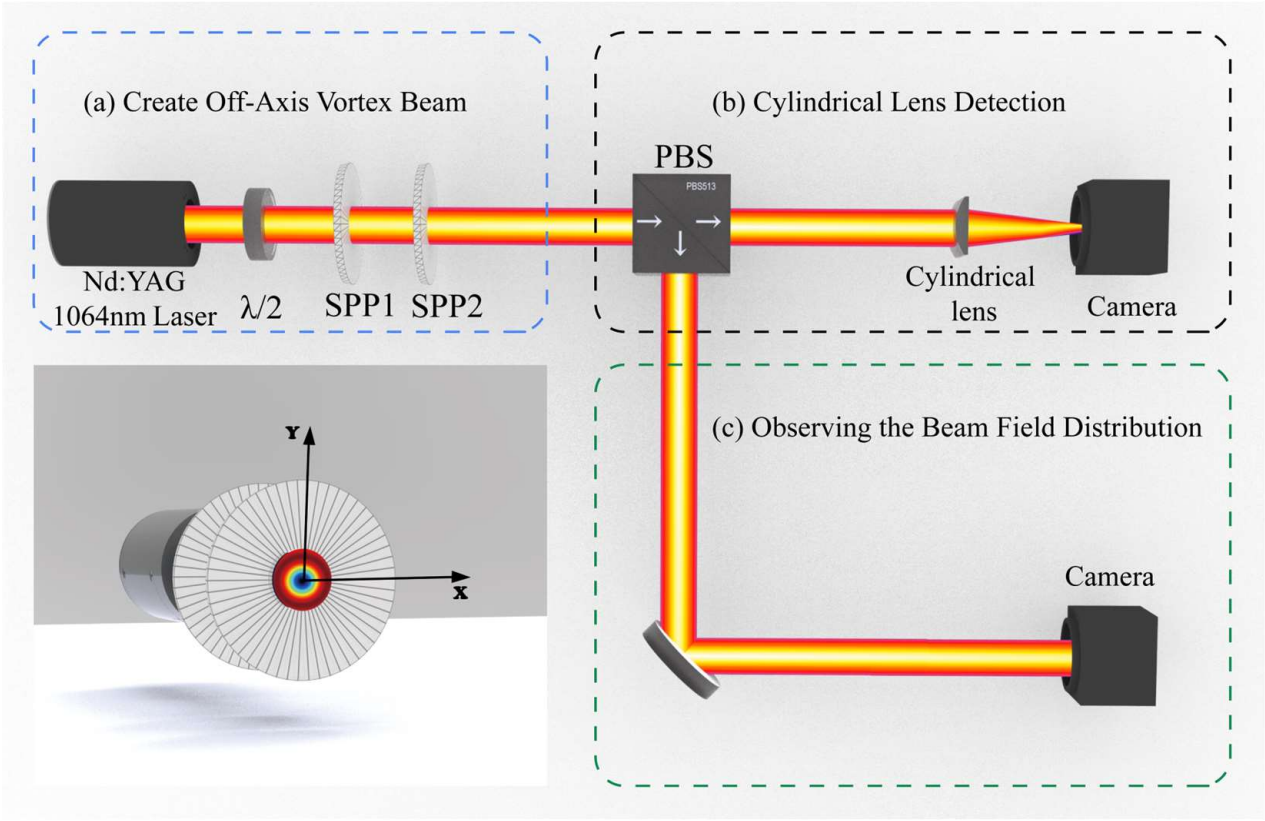

Figure 1. Schematic showing (**a**) the setup used to generate off-axis double vortex beams; (**b**) the setup using a cylindrical lens to determine the OAM content of the generated beams; and (**c**) the setup using a conventional CCD camera to observe the beam intensity distribution. Shown inset are schematic images of the two superimposed spiral phase plates (SPPs) used in this work.

3.1. Spatial Profile of Off-Axis Double Vortex Beams

Figure 2 shows a collection of spatial distributions of both theoretically (left most set) and experimentally (right most set) derived, off-axis vortex beams with different order and off-axis displacements. It can be seen that both the experimental results and modelled results are in agreement with one another, thus providing strong evidence for the accuracy of the theoretical equations and modelling. In each of the image sets, the columns from left to right represent an increase in the off-axis displacement (starting from zero displacement, i.e., on-axis) of SPP2 in the positive X and Y directions (to the top right, as outlined in the inset of Figure 1, and positive Δx and Δy values in the theoretical equations).

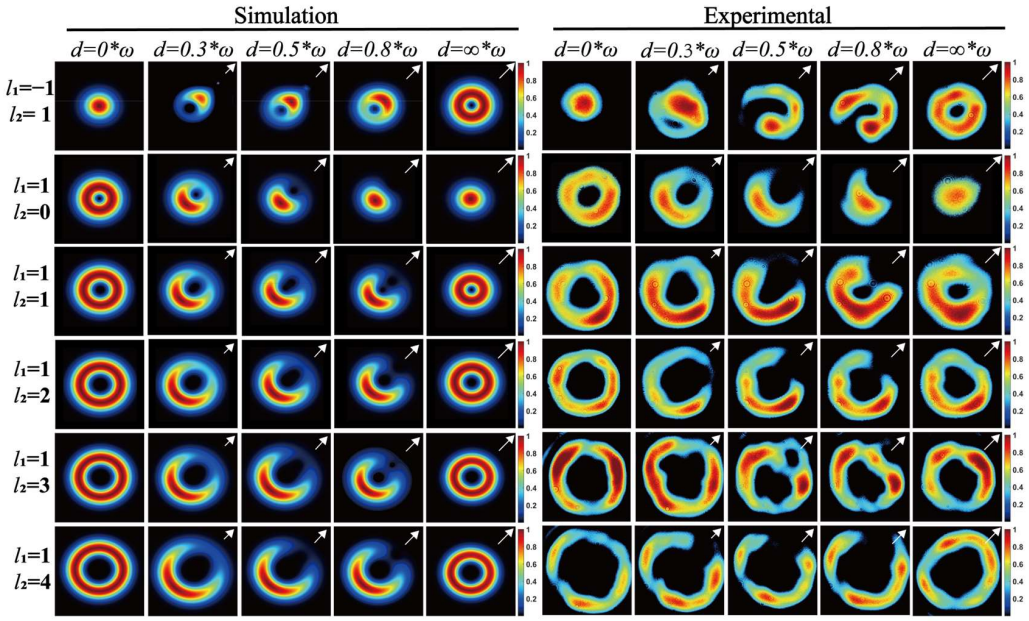

Figure 2. Sets of images showing the intensity distribution of theoretically modelled (left set) and experimentally generated (right set) off-axis double vortex beams (with different combinations of OAM) for a range of off-axis displacements. In each set of images, the columns from left to right represent increasing off-axis displacement (in the positive x and y directions). The OAM orders of the reference beams are 0–4, and the embedded beams have OAM orders of +1 and −1. The white arrows annotated in the figure indicate the direction of off-axis displacement, d represents the value of displacement in the off-axis direction and ω denotes the beam radius of integer vortex beams with different orders.

From the results, it can be observed that when $l_1 = -1$ and $l_2 = +1$, and there is no off-axis displacement, the intensity distribution resembles a Gaussian mode. As the off-axis displacement increases (in the upper–right direction), the intensity distribution becomes asymmetric with the appearance of a singularity and the formation of a radial notch in the direction opposite to the off-axis displacement. As the off-axis displacement increases, the position of the singularity becomes increasingly centralized until the overall beam resembles a 1st-order vortex beam.

When $l_1 = 1$ and $l_2 = 0$, with increasing off-axis displacement, the once centralized singularity now appears to propagate to the upper–right of the beam profile and gradually disappears, leaving a Gaussian beam. When $l_1 = 1$ and $l_2 = 1$, and there is no off-axis displacement, the beam is annular with an OAM order of $l_1 + l_2$ (i.e., 2 in this case). Similar to the $l_1 = 1$ and $l_2 = 0$ case, when off-axis displacement occurs, the annular shape of the beam is destroyed; however, in contrast, we observe a clear separation of two singularities. As the off-axis displacement increases, one of the singularities progresses out of the beam profile, leaving a vortex beam with an annular profile and OAM order of one. A similar characteristic is observed in the other data sets presented in Figure 2 and will not be further described in detail.

The topological charge of conventional vortex beams, represented by the constant integer value 'l', is exclusively determined by the beam's azimuthal index l. However, the orthogonal angular momentum (OAM) carried by these beams can change with off-axis displacement. Here, the topological charge remains constant while the average OAM experiences modulation as a result of the off-axis displacement. To overcome this limitation, we utilized the cylindrical lens transformation method which transforms the vortex beam into a multi-lobed beam with the lobes being indicative of the average OAM of the beam.

3.2. Cylindrical Lens Focusing Patterns of Off-Axis Double Vortex Beams

The cylindrical lens can be used to transform the vortex beam in order to determine its OAM order. Here, the transformed beam has multiple lobes which are indicative of the input beam's OAM order [51]. Generally, when a beam with orbital angular momentum (OAM) is focused, the number of lobes that appear is equal to the input beam's OAM order l plus one; this method allows for a simple and quick determination of the OAM order of the input beam. Theoretically, this can be understood by taking the Fourier transform and considering the phase of the cylindrical lens, which can be described as follows:

$$phi_c = 2\pi * \frac{f - \sqrt{|f|^2 + |y|^2}}{\lambda} \tag{6}$$

where f is the focal length of the cylindrical lens and λ is the wavelength of the incident beam.

Figure 3 shows sets of spatial profiles of the transformed vortex beams under propagation through a cylindrical lens of focal length = 300 mm. Similar to the sets of data presented in Figure 2, the left most set was obtained through theoretical modelling, while the right most set was obtained experimentally. In each set, the columns of images from left to right represent an increasing displacement in the positive X and Y directions. In each case, the modelled and experimental data sets correlate well with one another and the change in lobe patterns formed by focusing the vortex beam using the cylindrical lens are similar. In general, a vortex beam of order l forms (l + 1) lobes after being focused by a cylindrical lens. For off-axis double vortex beams, the generation of off-axis displacement causes the annular structure of the optical vortex to be broken and no longer maintain integrity, resulting in the intensity distribution formed by focusing through the cylindrical lens also no longer maintaining its centrosymmetry, and thus the upper end lobe intensity gradually weakens and finally merges into the lower-level lobe. When the off-axis displacement is small, only the outermost lobe is affected, and as the off-axis displacement increases, the intensity of the outermost lobe gradually decreases until it is eventually absorbed by the inner lobes. The cylindrical lens transformation method was effective at examining the OAM characteristics of higher-order vortex beams.

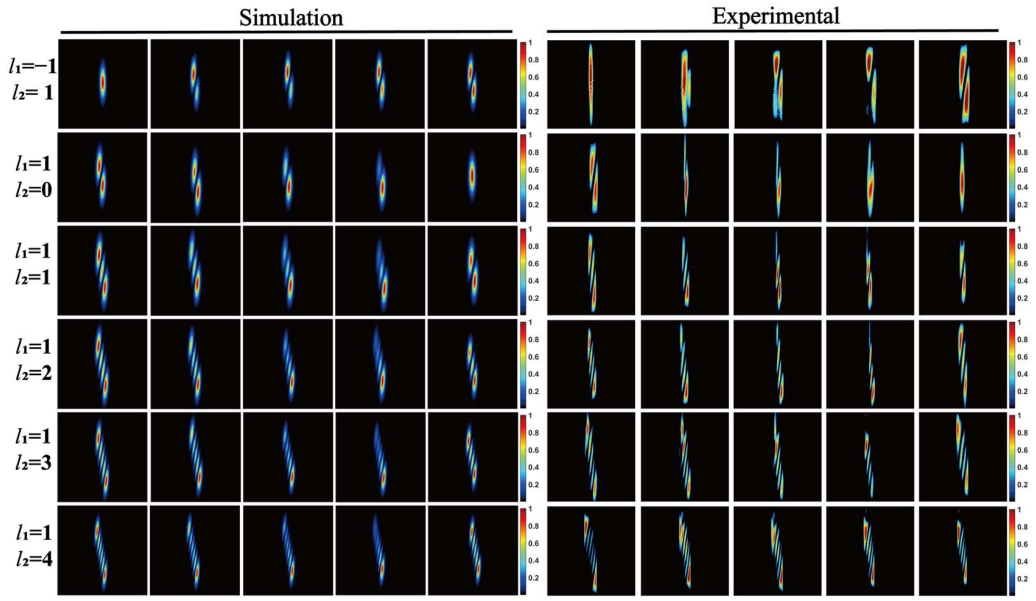

Figure 3. Images showing the theoretically modelled (left set) and experimentally obtained (right set) vortex beam profiles upon propagation through a cylindrical lens. Images are shown for a range of OAM values and progressively increasing off-axis displacement (columns from left to right in each set).

4. Conclusions

In this study, we derived the equations describing off-axis double vortex beams and used these to theoretically simulate the spatial profiles of these beams. Experiments were also performed wherein these off-axis double vortex beams were generated through the transformation of a Gaussian laser beam using two spiral phase plates. By changing the off-axis alignment of these two spiral phase plates, we were able to manipulate both the spatial form and OAM of the generated off-axis vortex beams. The OAM content of these beams was determined using cylindrical lens transformation techniques. We anticipate that the methods detailed in this work can be further applied to the modelling and generation of off-axis triple (and higher) vortex beams; beams which may have great utility in cutting-edge, high-density communications and high-order micro-manipulation applications.

Author Contributions: Conceptualization, J.Y. and T.Y.; methodology, J.Y. and T.Y.; software, J.Y.; validation, J.Y., T.Y. and Y.Z.; formal analysis, J.Y. and P.A.; investigation, J.Y.; resources, Y.Z.; data curation, Y.Z. and Z.L.; writing—original draft preparation, J.Y., X.Y. and T.Y.; writing—review and editing, T.Y., X.Y. and Z.L.; visualization, J.Y.; supervision T.Y. and Z.L.; project administration and funding acquisition, T.Y. All authors have read and agreed to the published version of the manuscript.

Funding: This research was funded by the National Natural Science Foundation of China (Grant Nos. 12264049 and 11664041), the Natural Science Foundation of the Xinjiang Uygur Autonomous (Grant No. 2021D01A114) and the Xinjiang Normal University Young Outstanding Talent Programmer (Grant No. XJNUQB2022-17).

Institutional Review Board Statement: Not applicable.

Informed Consent Statement: Not applicable.

Data Availability Statement: The data underlying the results presented in this paper are not publicly available at this time but may be obtained from the authors upon reasonable request.

Conflicts of Interest: The authors declare no conflicts of interest.

References

1. Allen, L.; Beijersbergen, M.W.; Spreeuw, R.J.C.; Woerdman, J.P. Orbital Angular Momentum of Light and the Transformation of Laguerre-Gaussian Laser Modes. *Phys. Rev. A* **1992**, *45*, 8185–8189. [CrossRef]
2. Ruffato, G.; Massari, M.; Romanato, F. Generation of High-Order Laguerre–Gaussian Modes by Means of Spiral Phase Plates. *Opt. Lett.* **2014**, *39*, 5094–5097. [CrossRef] [PubMed]
3. JJ Nivas, J.; He, S.; Rubano, A.; Vecchione, A.; Paparo, D.; Marrucci, L.; Bruzzese, R.; Amoruso, S. Direct Femtosecond Laser Surface Structuring with Optical Vortex Beams Generated by a Q-Plate. *Sci. Rep.* **2015**, *5*, 17929. [CrossRef]
4. Wu, Y.; Wen, J.; Zhang, M.; Wen, J.; Chen, W.; Zhang, X.; Pang, F.; Tang, F.; West, G.; Wang, T. Over 100 Nm Bandwidth Orbital Angular Momentum Modes Amplification for MDM and WDM Transmission with a Ring-Core Bi/Er Co-Doped Fiber. *J. Light. Technol.* **2022**, *40*, 7922–7929. [CrossRef]
5. Wu, Y.; Wen, J.; Tang, F.; Pang, F.; Guo, H.; Huang, S.; Wang, T. Orbital-Angular-Momentum Fluorescence Emission Based on Photon–Electron Interaction in a Vortex Field of an Active Optical Fiber. *Nanophotonics* **2023**, *12*, 43–53. [CrossRef]
6. Wu, Y.; Wen, J.; Zhang, M.; Cao, Y.; Chen, W.; Zhang, X.; Yusufu, T.; Pang, F.; Wang, T. Low-Loss and Helical-Phase-Dependent Selective Excitation of High-Order Orbital Angular Momentum Modes in a Twisted Ring-Core Fiber. *Opt. Lett.* **2022**, *47*, 4016–4019. [CrossRef]
7. Clark, T.W.; Offer, R.F.; Franke-Arnold, S.; Arnold, A.S.; Radwell, N. Comparison of Beam Generation Techniques Using a Phase Only Spatial Light Modulator. *Opt. Express* **2016**, *24*, 6249–6264. [CrossRef]
8. Goorden, S.A.; Bertolotti, J.; Mosk, A.P. Superpixel-Based Spatial Amplitude and Phase Modulation Using a Digital Micromirror Device. *Opt. Express* **2014**, *22*, 17999–18009. [CrossRef]
9. Marrucci, L.; Manzo, C.; Paparo, D. Optical Spin-to-Orbital Angular Momentum Conversion in Inhomogeneous Anisotropic Media. *Phys. Rev. Lett.* **2006**, *96*, 163905. [CrossRef]
10. Khonina, S.N.; Kotlyar, V.V.; Skidanov, R.V.; Soifer, V.A.; Laakkonen, P.; Turunen, J. Gauss–Laguerre Modes with Different Indices in Prescribed Diffraction Orders of a Diffractive Phase Element. *Opt. Commun.* **2000**, *175*, 301–308. [CrossRef]
11. Zhang, H.; Zeng, J.; Lu, X.; Wang, Z.; Zhao, C.; Cai, Y. Review on Fractional Vortex Beam. *Nanophotonics* **2022**, *11*, 241–273. [CrossRef]
12. Berry, M.V. Optical Vortices Evolving from Helicoidal Integer and Fractional Phase Steps. *J. Opt. A Pure Appl. Opt.* **2004**, *6*, 259. [CrossRef]

13. Hebri, D.; Rasouli, S.; Dezfouli, A.M. Theory of Diffraction of Vortex Beams from Structured Apertures and Generation of Elegant Elliptical Vortex Hermite–Gaussian Beams. *J. Opt. Soc. Am. A* **2019**, *36*, 839–852. [CrossRef] [PubMed]
14. Chen, Y.F.; Lai, Y.H.; Hsieh, M.X.; Hsieh, Y.H.; Tu, C.W.; Liang, H.C.; Huang, K.F. Wave Representation for Asymmetric Elliptic Vortex Beams Generated from the Astigmatic Mode Converter. *Opt. Lett.* **2019**, *44*, 2028–2031. [CrossRef] [PubMed]
15. Tkachenko, G.; Chen, M.; Dholakia, K.; Mazilu, M. Is It Possible to Create a Perfect Fractional Vortex Beam? *Optica* **2017**, *4*, 330–333. [CrossRef]
16. Zhou, Q.; Liu, M.; Zhu, W.; Chen, L.; Ren, Y.; Lezec, H.J.; Lu, Y.; Agrawal, A.; Xu, T. Generation of Perfect Vortex Beams by Dielectric Geometric Metasurface for Visible Light. *Laser Photonics Rev.* **2021**, *15*, 2100390. [CrossRef]
17. Yusufu, T.; Tokizane, Y.; Yamada, M.; Miyamoto, K.; Omatsu, T. Tunable 2-μm Optical Vortex Parametric Oscillator. *Opt. Express* **2012**, *20*, 23666–23675. [CrossRef]
18. Aadhi, A.; Samanta, G.K.; Kumar, S.C.; Ebrahim-Zadeh, M. Controlled Switching of Orbital Angular Momentum in an Optical Parametric Oscillator. *Optica* **2017**, *4*, 349–355. [CrossRef]
19. Omatsu, T.; Miyamoto, K.; Lee, A.J. Wavelength-Versatile Optical Vortex Lasers. *J. Opt.* **2017**, *19*, 123002. [CrossRef]
20. Niu, S.; Wang, S.; Ababaike, M.; Yusufu, T.; Miyamoto, K.; Omatsu, T. Tunable Near- and Mid-Infrared (1.36–1.63 μm and 3.07–4.81 μm) Optical Vortex Laser Source. *Laser Phys. Lett.* **2020**, *17*, 045402. [CrossRef]
21. Ababaike, M.; Wang, S.; Aierken, P.; Omatsu, T.; Yusufu, T. Near and Mid-Infrared Optical Vortex Parametric Oscillator Based on KTA. *Sci. Rep.* **2021**, *11*, 8013. [CrossRef] [PubMed]
22. Zhou, Y.; Yusufu, T.; Ma, Y.; Omatsu, T. Generation of Tunable, Non-Integer OAM States from an Optical Parametric Oscillator. *Appl. Phys. Lett.* **2023**, *122*, 121106. [CrossRef]
23. Yusufu, T.; Niu, S.; Tuersun, P.; Tulake, Y.; Miyamoto, K.; Omatsu, T. Tunable 3 μm Optical Vortex Parametric Oscillator. *Jpn. J. Appl. Phys.* **2018**, *57*, 122701. [CrossRef]
24. Abulikemu, A.; Yakufu, S.; Zhou, Y.X.; Yusufu, T. Mid-Infrared Idler-Resonant Optical Vortex Parametric Oscillator Based on MgO:PPLN. *Opt. Laser Technol.* **2024**, *171*, 110341. [CrossRef]
25. Zhu, L.; Tang, M.; Li, H.; Tai, Y.; Li, X. Optical Vortex Lattice: An Exploitation of Orbital Angular Momentum. *Nanophotonics* **2021**, *10*, 2487–2496. [CrossRef]
26. Qiao, Z.; Wan, Z.; Xie, G.; Wang, J.; Qian, L.; Fan, D. Multi-Vortex Laser Enabling Spatial and Temporal Encoding. *PhotoniX* **2020**, *1*, 13. [CrossRef]
27. Shao, W.; Huang, S.; Liu, X.; Chen, M. Free-Space Optical Communication with Perfect Optical Vortex Beams Multiplexing. *Opt. Commun.* **2018**, *427*, 545–550. [CrossRef]
28. Ding, D.-S.; Zhang, W.; Zhou, Z.-Y.; Shi, S.; Xiang, G.-Y.; Wang, X.-S.; Jiang, Y.-K.; Shi, B.-S.; Guo, G.-C. Quantum Storage of Orbital Angular Momentum Entanglement in an Atomic Ensemble. *Phys. Rev. Lett.* **2015**, *114*, 050502. [CrossRef]
29. Ndagano, B.; Nape, I.; Cox, M.A.; Rosales-Guzman, C.; Forbes, A. Creation and Detection of Vector Vortex Modes for Classical and Quantum Communication. *J. Light. Technol.* **2018**, *36*, 292–301. [CrossRef]
30. Tan, P.S.; Yuan, X.-C.; Yuan, G.H.; Wang, Q. High-Resolution Wide-Field Standing-Wave Surface Plasmon Resonance Fluorescence Microscopy with Optical Vortices. *Appl. Phys. Lett.* **2010**, *97*, 241109. [CrossRef]
31. Popiołek-Masajada, A.; Masajada, J.; Szatkowski, M. Internal Scanning Method as Unique Imaging Method of Optical Vortex Scanning Microscope. *Opt. Lasers Eng.* **2018**, *105*, 201–208. [CrossRef]
32. Zheng, C.; Li, H.; Zang, H.; Yao, J. Terahertz Polarization Detection Based on the Mode Analysis of Longitudinally Polarized Vortices. *Opt. Laser Technol.* **2024**, *170*, 110210. [CrossRef]
33. Zheng, C.; Liu, J.; Li, H.; Wang, M.; Zang, H.; Zhang, Y.; Yao, J. Terahertz Metasurface Polarization Detection Employing Vortex Pattern Recognition. *Photon. Res.* **2023**, *11*, 2256–2263. [CrossRef]
34. Toyoda, K.; Miyamoto, K.; Aoki, N.; Morita, R.; Omatsu, T. Using Optical Vortex to Control the Chirality of Twisted Metal Nanostructures. *Nano Lett.* **2012**, *12*, 3645–3649. [CrossRef] [PubMed]
35. Hnatovsky, C.; Shvedov, V.G.; Krolikowski, W.; Rode, A.V. Materials Processing with a Tightly Focused Femtosecond Laser Vortex Pulse. *Opt. Lett.* **2010**, *35*, 3417–3419. [CrossRef] [PubMed]
36. Zhou, Z.-Y.; Li, Y.; Ding, D.-S.; Zhang, W.; Shi, S.; Shi, B.-S. Optical Vortex Beam Based Optical Fan for High-Precision Optical Measurements and Optical Switching. *Opt. Lett.* **2014**, *39*, 5098–5101. [CrossRef] [PubMed]
37. Leach, J.; Yao, E.; Padgett, M.J. Observation of the Vortex Structure of a Non-Integer Vortex Beam. *New J. Phys.* **2004**, *6*, 71. [CrossRef]
38. Fang, Y.; Lu, Q.; Wang, X.; Zhang, W.; Chen, L. Fractional-Topological-Charge-Induced Vortex Birth and Splitting of Light Fields on the Submicron Scale. *Phys. Rev. A* **2017**, *95*, 023821. [CrossRef]
39. Maji, S.; Jacob, P.; Brundavanam, M.M. Geometric Phase and Intensity-Controlled Extrinsic Orbital Angular Momentum of Off-Axis Vortex Beams. *Phys. Rev. Appl.* **2019**, *12*, 054053. [CrossRef]
40. Gao, B.; Wen, J.; Zhu, G.; Ye, L.; Wang, L.-G. Precise Measurement of Trapping and Manipulation Properties of Focused Fractional Vortex Beams. *Nanoscale* **2022**, *14*, 3123–3130. [CrossRef]
41. Huang, K.; Liu, H.; Restuccia, S.; Mehmood, M.Q.; Mei, S.-T.; Giovannini, D.; Danner, A.; Padgett, M.J.; Teng, J.-H.; Qiu, C.-W. Spiniform Phase-Encoded Metagratings Entangling Arbitrary Rational-Order Orbital Angular Momentum. *Light Sci. Appl.* **2018**, *7*, 17156. [CrossRef]

42. Götte, J.B.; O'Holleran, K.; Preece, D.; Flossmann, F.; Franke-Arnold, S.; Barnett, S.M.; Padgett, M.J. Light Beams with Fractional Orbital Angular Momentum and Their Vortex Structure. *Opt. Express* **2008**, *16*, 993–1006. [CrossRef] [PubMed]
43. Kotlyar, V.V.; Kovalev, A.A.; Porfirev, A.P. Asymmetric Gaussian Optical Vortex. *Opt. Lett.* **2017**, *42*, 139–142. [CrossRef] [PubMed]
44. Anzolin, G.; Tamburini, F.; Bianchini, A.; Barbieri, C. Method to Measure Off-Axis Displacements Based on the Analysis of the Intensity Distribution of a Vortex Beam. *Phys. Rev. A* **2009**, *79*, 033845. [CrossRef]
45. Guo, M.; Le, W.; Wang, C.; Rui, G.; Zhu, Z.; He, J.; Gu, B. Generation, Topological Charge, and Orbital Angular Momentum of Off-Axis Double Vortex Beams. *Photonics* **2023**, *10*, 368. [CrossRef]
46. Mitri, F.G. Vector Spherical Quasi-Gaussian Vortex Beams. *Phys. Rev. E* **2014**, *89*, 023205. [CrossRef] [PubMed]
47. Mitri, F.G. Partial-Wave Series Expansions in Spherical Coordinates for the Acoustic Field of Vortex Beams Generated from a Finite Circular Aperture. *IEEE Trans. Ultrason. Ferroelectr. Freq. Control* **2014**, *61*, 2089–2097. [CrossRef] [PubMed]
48. Indebetouw, G. Optical Vortices and Their Propagation. *J. Mod. Opt.* **1993**, *40*, 73–87. [CrossRef]
49. Weng, X.; Miao, Y.; Wang, G.; Zhan, Q.; Dong, X.; Qu, J.; Gao, X.; Zhuang, S. Propagable Optical Vortices with Natural Noninteger Orbital Angular Momentum in Free Space. *Adv. Photonics Res.* **2023**, *4*, 2200094. [CrossRef]
50. Zeng, J.; Liu, X.; Wang, F.; Zhao, C.; Cai, Y. Partially Coherent Fractional Vortex Beam. *Opt. Express* **2018**, *26*, 26830–26844. [CrossRef]
51. Peng, Y.; Gan, X.-T.; Ju, P.; Wang, Y.-D.; Zhao, J.-L. Measuring Topological Charges of Optical Vortices with Multi-Singularity Using a Cylindrical Lens. *Chin. Phys. Lett.* **2015**, *32*, 024201. [CrossRef]